Beta interferon and gamma interferon synergize to block viral DNA and virion synthesis in herpes simplex virus-infected cells

Amy T. Pierce,[1] Joanna DeSalvo,[1] Timothy P. Foster,[2] Athena Kosinski,[3] Sandra K. Weller[3] and William P. Halford[4]

Correspondence
William P. Halford
halford@montana.edu

[1]Department of Microbiology and Immunology, Tulane University Medical School, New Orleans, LA 70112, USA

[2]Division of Biotechnology and Molecular Medicine, School of Veterinary Medicine, Louisiana State University, Baton Rouge, LA 70803, USA

[3]Department of Molecular, Microbial and Structural Biology, University of Connecticut Health Center, Farmington, CT 06030, USA

[4]Department of Veterinary Molecular Biology, Montana State University, 960 Technology Boulevard, Bozeman, MT 59718, USA

Received 18 February 2005
Accepted 10 June 2005

The capacity of herpes simplex virus type 1 (HSV-1) to replicate *in vitro* decreases tremendously when animal cell cultures are exposed to ligands of both the alpha/beta interferon (IFN-α/β) receptor and IFN-γ receptor prior to inoculation with low m.o.i.s of HSV-1. However, the available evidence provides no insight into the possible mechanisms by which co-activation of the IFN-α/β- and IFN-γ-signalling pathways produces this effect. Therefore, it has not been possible to differentiate between whether these observations represent an important *in vitro* model of host immunological suppression of HSV-1 infection or an irrelevant laboratory phenomenon. Therefore, the current study was initiated to determine whether co-activation of the host cell's IFN-α/β and IFN-γ pathways either (i) induced death of HSV-1-infected cells such that virus replication was unable to occur; or (ii) disrupted one or more steps in the process of HSV-1 replication. To this end, multiple steps in HSV-1 infection were compared in populations of Vero cells infected with HSV-1 strain KOS (m.o.i. of 2·5) and exposed to ligands of the IFN-α/β receptor, the IFN-γ receptor or both. The results demonstrated that IFN-β and IFN-γ interact in a synergistic manner to block the efficient synthesis of viral DNA and nucleocapsid formation in HSV-1-infected cells and do so without compromising host-cell viability. It was inferred that IFN-mediated suppression of HSV-1 replication may be a central mechanism by which the host immune system limits the spread of HSV-1 infection *in vivo*.

INTRODUCTION

Co-activation of the alpha/beta interferon (IFN-α/β)- and IFN-γ-signalling pathways produces a block in herpes simplex virus type 1 (HSV-1) replication of a magnitude that is not attainable with IFN-α/β or IFN-γ alone, and this effect is not cell type-, species- or virus strain-specific (Balish *et al.*, 1992; Chen *et al.*, 1994; Sainz & Halford, 2002). This observation has important ramifications because it suggests a previously unrecognized mechanism by which two cytokines of the immune system may cooperate to control HSV-1 infection non-cytolytically *in vivo*. Given that IFN-α/β and IFN-γ also act potently in concert to inhibit varicella-zoster virus (Desloges *et al.*, 2005), human cytomegalovirus (Sainz *et al.*, 2005) and the severe acute respiratory syndrome-associated coronavirus (Sainz *et al.*, 2004), the proposed interaction between the IFN-α/β- and IFN-γ-signalling pathways may be of general importance in host control of viral infections.

The available evidence indicates that an interaction between the IFN-α/β- and IFN-γ-signalling pathways is functionally relevant in host control of HSV-1 infections. Recent comparisons in knockout mice demonstrated that mice that lacked both IFN-α/β receptors and IFN-γ receptors (*IFN-*$\alpha/\beta R^{-/-}$ and *IFN-*$\gamma R^{-/-}$) were profoundly impaired in their resistance to HSV-1 strain KOS infection, experienced systemic viral spread and died 4–6 days after footpad inoculation (Luker *et al.*, 2003; Vollstedt *et al.*, 2004). This phenotype is in stark contrast to single-receptor knockout mice (*IFN-*$\alpha/\beta R^{-/-}$ or *IFN-*$\gamma R^{-/-}$), which retain their capacity to limit HSV-1 spread and often survive infection

with the KOS strain, despite the absence of one of the two IFN receptors (Luker *et al.*, 2003). Whilst these *in vivo* studies have established that loss of both IFN receptors has a catastrophic effect on host defence against HSV-1, they provide only limited insight into how the IFN-α/β and IFN-γ pathways normally interact to control the spread of HSV-1 infection.

The nature of the block in HSV-1 replication produced by IFN-α/β and IFN-γ remains undefined. Does exposure to IFN-α/β and IFN-γ cause host cells to undergo apoptosis upon HSV-1 infection (Park *et al.*, 2004; Takaoka *et al.*, 2003)? The low-multiplicity design of previous *in vitro* studies does not exclude this possibility (Balish *et al.*, 1992; Chen *et al.*, 1994; Sainz & Halford, 2002). Alternatively, IFN-β and IFN-γ may create a block in HSV-1 replication that does not compromise the viability of the host cell. If so, then at which step(s) between immediate-early (IE) mRNA transcription and virion egress does the inhibitory block occur? There are no published studies that address these questions.

The current study was initiated to refine our understanding of how co-activation of the IFN-α/β- and IFN-γ-signalling pathways prevents HSV-1 replication *in vitro*. Given the complexity of the HSV-1 replication cycle, we thought it unrealistic to test the scores of hypotheses that might explain the inhibitory effect sequentially. Rather, we felt that a more directed approach was first to constrain the number of possible explanations by determining whether IFN-β and IFN-γ are (i) cytotoxic to HSV-1 infected cells or (ii) disrupt HSV-1 replication at one or more discernible steps relative to viral mutants or an inhibitor of viral DNA synthesis. By using this approach, the separate versus combined effects of IFN-β and IFN-γ on viral DNA, mRNA, protein and virion accumulation were compared in Vero cells infected with 2·5 p.f.u. per cell of HSV-1. The use of an m.o.i. that infected nearly 100 % of cells in the population ensured that any differences in the measured parameters were the result of a defect in the first, and only, cycle of virus replication. We report that IFN-β and IFN-γ do not inhibit HSV-1 replication via a non-specific cytotoxic effect. Rather, IFN-β and IFN-γ render host cells non-permissive for viral DNA synthesis and nucleocapsid assembly, and thus suppress HSV-1 replication in the vast majority of infected cells.

METHODS

Cells, viruses and IFNs. Vero cells, ICP4-complementing E5 cells (DeLuca *et al.*, 1985), origin-binding protein (OBP)-complementing 2B.11 cells (Malik *et al.*, 1992) and glycoprotein D (gD)-complementing V15-D1 cells (Warner *et al.*, 1998) were propagated in Dulbecco's modified Eagle's medium (DMEM) supplemented with 5 % fetal bovine serum (FBS). Wild-type HSV-1 strain KOS (Smith, 1964) was propagated in Vero cells. The ICP4$^-$ virus n12 (kindly provided by Priscilla Schaffer, Harvard University, USA; DeLuca *et al.*, 1985), the OBP$^-$ virus hr94 (Malik *et al.*, 1992) and the gD$^-$ virus KOS-gD6 (kindly provided by Patricia Spear, Northwestern University, USA; Warner *et al.*, 1998) were propagated in their corresponding complementing cell lines. Aliquots of recombinant human IFN-β and human IFN-γ (PBL Biomedical Laboratories) were stored at $-80\,^{\circ}$C and diluted to 200 U ml^{-1} just prior to use. Combinations of IFN-β and IFN-γ (100 U ml^{-1} each) were made by mixing 200 U IFN-β ml^{-1} with 200 U IFN-γ ml^{-1} in a 1 : 1 ratio. Throughout this study, IFN treatment and KOS infection were performed by a standardized protocol. Culture dishes were seeded with Vero cells and cells were treated 24 h later with 200 U IFN-β ml^{-1}, 200 U IFN-γ ml^{-1} or 100 U each of IFN-β and IFN-γ ml^{-1}. Sixteen hours later, Vero cells were inoculated with virus at an m.o.i. of 2·5. After adsorption for 45 min, the inoculum was replaced with complete DMEM containing no IFN (vehicle), 200 U IFN-β ml^{-1}, 200 U IFN-γ ml^{-1}, 100 U each of IFN-β and IFN-γ ml^{-1} or 300 μM acyclovir.

Dot-blot analysis of HSV-1 DNA yield. Vero cells were established at a density of 1×10^5 cells per well in 24-well plates and infected with KOS at an m.o.i. of 2·5. Cultures were incubated in the presence of vehicle, 200 U IFN-β ml^{-1}, 200 U IFN-γ ml^{-1}, 100 U each of IFN-β and IFN-γ ml^{-1} or 300 μM acyclovir. Between 9 and 24 h post-infection (p.i.), crude DNA lysates were harvested and probed for viral DNA and the results were enumerated as described previously (Halford *et al.*, 2005a).

Flow cytometry

Enumeration of morphologically normal cells. Vero cells were established at a density of 2×10^5 cells per well in 12-well plates and infected with KOS at an m.o.i. of 2·5. Cultures were incubated in the presence of vehicle, 200 U IFN-β ml^{-1}, 200 U IFN-γ ml^{-1}, 100 U each of IFN-β and IFN-γ ml^{-1} or 300 μM acyclovir. Uninfected cells or KOS-infected cells were harvested by aspirating culture medium, rinsing with 1 ml PBS, dissociation in trypsin, resuspension in PBS with 10 % FBS and passing cells through a 50 μm mesh to remove cell debris. Cells were counted for a fixed period of time (2 min) on a FACSCalibur (BD Biosciences). At each time point, the total number of cells in four cultures was determined by using a haemocytometer and compared with the number of cells counted by the flow cytometer. On average, the flow cytometer counted ~40 % of cells in these cultures. Therefore, the total number of morphologically normal cells per culture was estimated by dividing the number of cells counted by the flow cytometer by the fraction of cells sampled (e.g. ~0·4).

Two-colour analysis of viral protein expression in HSV-1-infected cells. Vero cells were established at a density of $4{\cdot}5 \times 10^6$ cells per 100 mm dish and infected with KOS at an m.o.i. of 2·5. At 9 h p.i., Vero cells were dissociated with trypsin and prepared for immunofluorescent labelling by fixation in 2 % formaldehyde with 2 % sucrose, permeabilization in 90 % methanol, passage through a 27-gauge needle and resuspension in PBS plus 0·5 % FBS containing Fc-γ-receptor blocking agents (i.e. 5 μg each of human IgG, donkey IgG and goat IgG ml^{-1}). Cells were incubated for 1 h with a 1 : 20 000 dilution of rabbit anti-HSV-1 (Dako Cytomation) and a 1 : 1000 dilution of mouse mAb against ICP0, ICP4, ICP6, gC or gD (Rumbaugh Goodwin Institute). Cells were washed twice and incubated for 30 min with a 1 : 1000 dilution of phycoerythrin (PE)-labelled donkey anti-rabbit IgG and a 1 : 350 dilution of fluorescein isothiocyanate (FITC)-labelled goat anti-mouse IgG. Cells were washed twice and the fluorescent intensity of ~10 000 cells was measured in each sample (i.e. 10 000 events) by using a FACSCalibur and CellQuest Pro software (BD Biosciences). ICP8 was detected by the same methodology, but cells were labelled singly by incubating for 1 h with a 1 : 20 000 dilution of rabbit polyclonal anti-ICP8 antibody (generously donated by William Ruyechan, State University of New York, Buffalo, USA). For each viral protein, total protein yield was summed by multiplying the fraction of viral protein-positive

cells by the mean fluorescent intensity of viral protein staining and this 'fluorescent volume' was normalized relative to the lower limit of detection of the assay, which was defined as three times the background fluorescent volume associated with uninfected cells (Soboleski *et al.*, 2005).

Measurement of HSV-1 virion yields. Vero cells were established at a density of $4{\cdot}5 \times 10^6$ cells per dish in 100 mm dishes and infected with KOS at an m.o.i. of 2·5. Cultures were incubated in the presence of vehicle, 200 U IFN-β ml^{-1}, 200 U IFN-γ ml^{-1}, 100 U each of IFN-β and IFN-γ ml^{-1} or 300 μM acyclovir. Cells were prepared for transmission electron microscopy at 18 h p.i. as described previously (Foster *et al.*, 2003, 2004).

For analysis of virion yields, cells were transferred to −80 °C at 18 h p.i. and virion yields were determined in cell lysates following purification through a series of two gradients. For each sample, 15 fractions that spanned the 30–60 % sucrose interface of the second gradient were identified by using a refractometer, and virion yield in each fraction was measured by ELISA. Each fraction was diluted 1 : 10, 1 : 50 or 1 : 250 in PBS, and each dilution was used as coating antigen in two wells of a 96-well plate. After overnight incubation, virion fractions were discarded, wells were blocked with 0·5 % dried milk and a 1 : 600 dilution of anti-HSV-1 conjugated to horseradish peroxidase (Dako Cytomation) was added per well. After 1 h, excess antibody was rinsed away and bound antibody was measured with TMB Blue substrate (Dako Cytomation; A_{450}) in a plate reader.

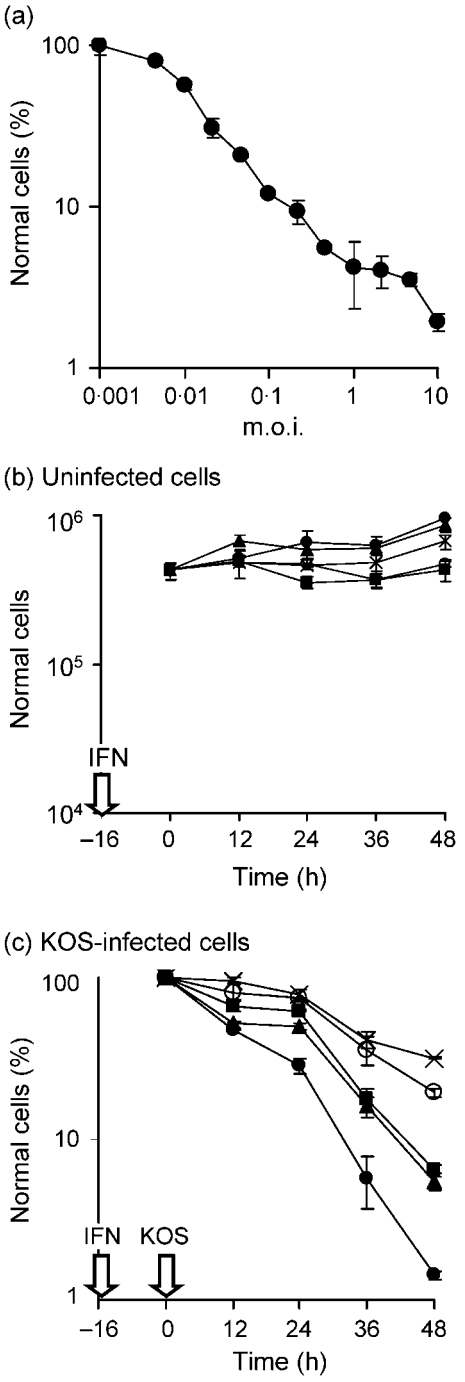

RESULTS

IFN-β and IFN-γ synergistically protect HSV-1-infected cells from viral cytopathic effect (CPE)

Flow cytometry was used to enumerate the number of morphologically normal cells per culture. The validity of the method was tested on Vero cells infected with m.o.i.s of 0·001–10 of HSV-1 strain KOS for 36 h. Flow cytometry confirmed that the fraction of normal cells decreased as viral m.o.i. increased (Fig. 1a) and the results correlated well with the degree of CPE observed by light microscopy. Treatment of Vero cell monolayers with 200 U IFN-β or IFN-γ ml^{-1}, 100 U each of IFN-β and IFN-γ ml^{-1} or 300 μM acyclovir had no effect on cell morphology (Fig. 1b). However, treatments that contained IFN-β prevented proliferation to the same extent as vehicle-treated cells. By comparison, other compounds used to inhibit HSV-1 replication, such as 10 μM MG132 (Poon *et al.*, 2002) or 100 μM roscovitine (Schang *et al.*, 1998), were overtly toxic to uninfected Vero cells within 24 h (not shown).

Infection with HSV-1 strain KOS (m.o.i. of 2·5) destroyed ~99 % of vehicle-treated cells by 48 h p.i. (Fig. 1c). Treatment with IFN-β or IFN-γ delayed the onset of CPE in KOS-infected cultures and increased the fraction of normal cells recovered between 24 and 48 h p.i. (Fig. 1c). Acyclovir or a combination of IFN-β and IFN-γ provided the greatest protection, such that, in these treatment groups, ~30 % of KOS-infected cells remained morphologically normal at

Fig. 1. IFN-β and IFN-γ protect HSV-1-infected cells from viral CPE. (a) The percentage of morphologically normal cells in HSV-1-infected cultures (relative to uninfected cultures) at 36 h p.i. plotted as a function of viral m.o.i. ($n=2$ per group). 'Normal' cells were defined as adherent cells that retained the forward and side-scatter properties of healthy, untreated Vero cells following dissociation with trypsin. (b) Uninfected cells per culture that remained morphologically normal at times after treatment with 300 μM acyclovir (ACV, ×), vehicle (●), 200 U IFN-β ml^{-1} (■), 200 U IFN-γ ml^{-1} (▲) or 100 U each of IFN-β and IFN-γ ml^{-1} (○). (c) Percentage of KOS-infected cells (m.o.i. of 2·5) that remained morphologically normal at times after inoculation in the presence of ACV (×), vehicle (●), IFN-β (■), IFN-γ (▲) or IFN-β and IFN-γ (○).

48 h p.i. (Fig. 1c). Therefore, treatment with IFN-β and/or IFN-γ was not cytotoxic to Vero cells, but rather delayed the onset of viral CPE in KOS-infected cells.

IFN-β and IFN-γ synergistically reduce the efficiency of HSV-1 DNA synthesis

The combined versus separate effects of IFN-β and IFN-γ on HSV-1 DNA synthesis were compared in Vero cells inoculated with HSV-1 strain KOS (m.o.i. of 2·5). DNA samples harvested at 9–24 h p.i. were immobilized on a nylon membrane and hybridized to a probe specific for the HSV-1 US6 gene (Fig. 2a). Treatment with 200 U IFN-β or IFN-γ ml^{-1} alone delayed the detection of viral DNA synthesis by approximately 3 h and slightly decreased the rate (slope) of viral DNA synthesis between 15 and 24 h p.i. relative to vehicle-treated controls (Fig. 2a and b). Combined treatment with 100 U each of IFN-β and IFN-γ ml^{-1} delayed the detection of viral DNA synthesis by 6 h and greatly reduced the rate of HSV-1 DNA synthesis (Fig. 2a and b; $P<0{\cdot}001$, as determined by one-way ANOVA and Tukey's post hoc t-test). Unlike IFN-β and IFN-γ, which only reduced the efficiency of HSV-1 DNA synthesis, 300 μM acyclovir prevented the detection of HSV-1 DNA synthesis completely (Fig. 2a and b).

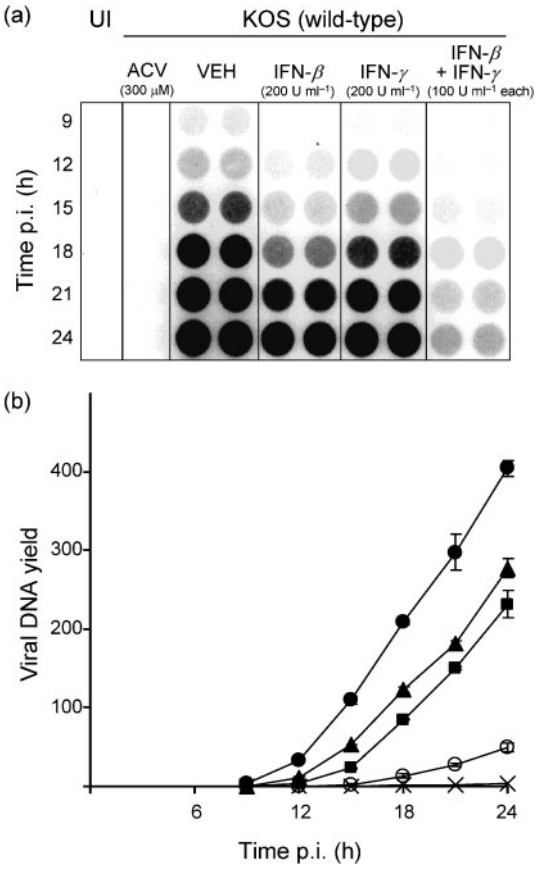

Fig. 2. Effect of IFN-β and IFN-γ on viral DNA levels. (a) Dot blot of DNA from uninfected (UI) cells and KOS-infected Vero cells treated with 300 μM ACV, vehicle (VEH), 200 U IFN-β ml^{-1}, 200 U IFN-γ ml^{-1} or 100 U each of IFN-β and IFN-γ ml^{-1}. DNA was harvested at 9–24 h after infection with 2·5 p.f.u. KOS per cell and was hybridized to a US6-specific probe. (b) Viral DNA yield in each group was plotted as a function of time. Symbols and error bars indicate the mean ± SEM of measurements of log(viral DNA yield), which are expressed in terms of log(fold increase above the lower limit of detection). Thus, zero on the y axis indicates the lower limit of detection of the assay [i.e. 0 = log(1 × lower limit of detection)]. ×, ACV; ●, vehicle; ■, IFN-β; ▲, IFN-γ; ○, IFN-β+IFN-γ.

IFN-β and IFN-γ synergistically reduce the accumulation of HSV-1 mRNAs

The combined versus separate effects of IFN-β and IFN-γ on HSV-1 mRNA synthesis were compared in Vero cells inoculated with HSV-1 strain KOS (m.o.i. of 2·5). RNA samples harvested at 9 h after inoculation were compared by Northern blot analysis. In vehicle-treated cells, KOS infection reduced the amount of probe that hybridized to cellular glyceraldehyde-3-phosphate dehydrogenase (G3PDH) mRNA to 15 % of that observed in uninfected Vero cells (Fig. 3). In KOS-infected cells treated with IFN-β or IFN-γ, G3PDH mRNA levels were ~50 % of normal levels. However, G3PDH mRNA levels remained at 100 % of normal levels in KOS-infected cells treated with IFN-β and IFN-γ or with 300 μM acyclovir (Fig. 3). Northern blot analysis of viral IE or early (E) mRNAs revealed that IFN-β or IFN-γ had little effect on the abundance of ICP4, ICP27, ICP0 or HSV DNA polymerase (pol) mRNAs in KOS-infected Vero cells (Fig. 3). However, treatment with IFN-β and IFN-γ or with 300 μM acyclovir reduced the amount of probe that hybridized to ICP4, ICP27, ICP0 and pol mRNAs by two- to threefold (Fig. 3). Treatment with IFN-β or IFN-γ alone caused a one- to threefold reduction in the amount of probe that hybridized to viral late (L) mRNAs that encoded VP5, VP23 or gD (Fig. 3). Treatment with IFN-β and IFN-γ or with 300 μM acyclovir caused a five- to 10-fold reduction in the amount of probe that hybridized to these L viral mRNAs (Fig. 3). The degree to which IFN-β and IFN-γ reduced viral mRNA levels was equivalent to that achieved by 300 μM acyclovir. Thus, the acyclovir control suggested that a block in the amplification of the number of genomes available for mRNA synthesis might contribute significantly to the reduced viral mRNA levels observed in KOS-infected cells treated with IFN-β and IFN-γ.

IFN-β and IFN-γ synergistically reduce the accumulation of HSV-1 proteins

Flow cytometry was used to compare the combined versus separate effects of IFN-β and IFN-γ on the expression of individual HSV-1 proteins in Vero cells inoculated with KOS (m.o.i. of 2·5). Cells were labelled doubly with mAbs against individual viral proteins (e.g. ICP0, ICP4, ICP6 or gD) and rabbit polyclonal antibody against HSV-1, which served as an internal control for the consistency of antibody labelling. Irrelevant mouse antibodies or irrelevant rabbit antibodies failed to label KOS-infected cells (not shown). As

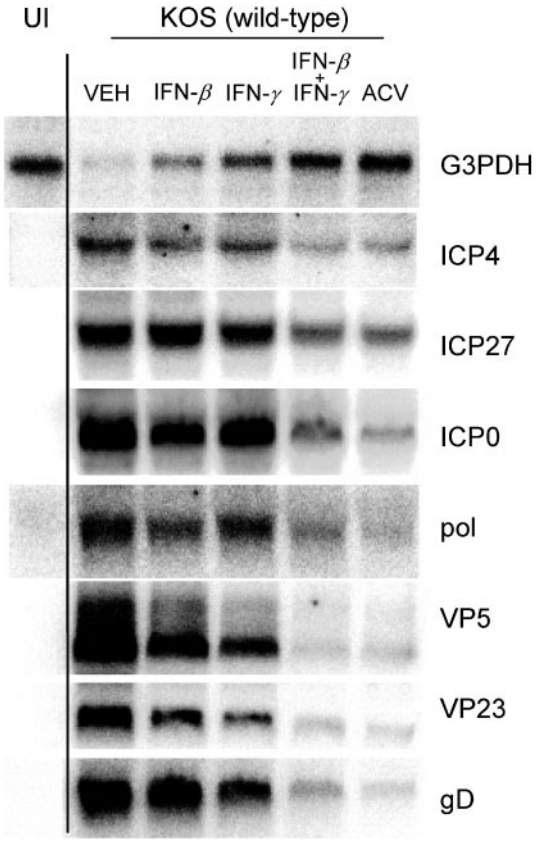

Fig. 3. Effect of IFN-β and IFN-γ on viral mRNA levels. Northern blot analysis of Vero-cell RNA harvested at 9 h p.i. from uninfected cells (UI) or from cells infected with 2·5 p.f.u. KOS per cell and hybridized to radiolabelled probes specific for mRNAs encoding cellular G3PDH or viral ICP4, ICP27, ICP0, HSV-1 DNA polymerase (pol), VP5, VP23 or glycoprotein D (gD), as indicated. KOS-infected Vero cells were treated with vehicle (VEH), 200 U IFN-β ml^{-1}, 200 U IFN-γ ml^{-1}, 100 U each of IFN-β and IFN-γ ml^{-1} or 300 μM ACV.

expected, the ICP4$^-$ virus n12 expressed high levels of ICP0 (Fig. 4a and b) and the N-terminal 251 aa of ICP4 (DeLuca & Schaffer, 1987), to which the ICP4 antibody binds (Hubenthal-Voss *et al.*, 1988) (Fig. 4c and d). The ICP4$^-$ virus expressed only low levels of ICP6 (Fig. 4e and f) and undetectable levels of gD (Fig. 4g and h). In contrast, OBP$^-$ and gD$^-$ viruses expressed high levels of these viral proteins (Fig. 4a–f) with the exception of the gD$^-$ virus, which failed to express gD (Fig. 4g and h).

KOS-infected cells treated with vehicle expressed the IE proteins ICP0 and ICP4 at levels that were 80- and 130-fold above the lower limit of detection (Fig. 4a and c). Treatment with 200 U IFN-β ml^{-1} or 200 U IFN-γ ml^{-1} reduced ICP0 and ICP4 abundance by 1·1- to 1·8-fold relative to vehicle-treated cells, whereas 100 U ml^{-1} each of IFN-β and IFN-γ reduced ICP0 and ICP4 abundance by 2·5- and 3·3-fold, respectively (Fig. 4a and c). Most of the change in ICP0 and ICP4 abundance was not due to differences in protein level per cell (as measured by mean fluorescent intensity), but rather was due to the fact that IFN-β and IFN-γ decreased the frequency of KOS-infected cells that were ICP0$^+$ or ICP4$^+$ by 70 and 60 %, respectively (Fig. 4b and d). IFN-β and IFN-γ caused a 5·1-fold reduction in the abundance of the E protein ICP6 relative to vehicle-treated cells (Fig. 4e), which was largely attributable to a 75 % decrease in the frequency of ICP6$^+$ cells (Fig. 4f). Analysis of ICP8 expression (an E protein) revealed a similar pattern (not shown). IFN-β and IFN-γ caused a 7·0-fold reduction in the abundance of the leaky L protein gD relative to vehicle-treated, KOS-infected cells (Fig. 4g). This decrease was not only due to a 75 % decrease in the frequency of gD$^+$ cells (Fig. 4h), but was also compounded by a 45 % reduction in gD protein per cell (as measured by mean fluorescent intensity). IFN-β and IFN-γ caused a 27-fold reduction in the abundance of the true L protein gC relative to vehicle-treated, KOS-infected cells (not shown). This decrease was due to a 94 % decrease in the frequency of gC$^+$ cells and a 40 % reduction in gC protein per cell. Flow-cytometric analysis suggested that IFN-β and IFN-γ acted at two levels to (i) prevent detectable viral IE and E protein synthesis in ~70 % of KOS-infected cells (e.g. as measured by reduced frequency of ICP0$^+$ cells) and (ii) restrict virus replication in the remaining ~30 % of KOS-infected cells in a manner that did not affect viral IE and E protein synthesis.

The full inhibitory effect of IFN-β and IFN-γ is achieved before or during viral DNA synthesis

Vero cells were infected with HSV-1 strain KOS (m.o.i. of 2·5) and treated with vehicle, IFN-β, IFN-γ, IFN-β and IFN-γ, or 0·3–320 μM acyclovir. Cultures were harvested at 18 h p.i. to compare viral DNA yields (Fig. 5a and b) and viral titres (Fig. 5c). Relative to vehicle-treated cells, a combination of IFN-β and IFN-γ reduced HSV-1 DNA yields in KOS-infected cells by ~100-fold, which was equivalent to the reduction achieved by 32 μM acyclovir (Fig. 5a and b). The same combination of IFN-β and IFN-γ reduced infectious viral titres by ~1000-fold relative to vehicle-treated cells and 32 μM acyclovir was found to reduce viral titres to precisely the same extent (Fig. 5c). Regression analysis of viral titres versus DNA yield confirmed that acyclovir, an acyclic guanosine analogue (Elion, 1983), reduced HSV-1 titres in direct proportion to the drug's inhibitory effect on viral DNA synthesis (closed circles in Fig. 5d). Likewise, it was observed that IFN-β alone, IFN-γ alone or IFN-β and IFN-γ each reduced HSV-1 titres in direct proportion to their inhibitory effects on HSV-1 DNA synthesis (open symbols in Fig. 5d). Therefore, the results suggested that IFN-β and/or IFN-γ must achieve their full inhibitory effect on HSV-1 replication before or during the process of viral DNA synthesis.

IFN-β and IFN-γ synergistically inhibit HSV-1 virion synthesis

The combined versus separate effects of IFN-β and IFN-γ on HSV-1 virion synthesis were compared in Vero cells

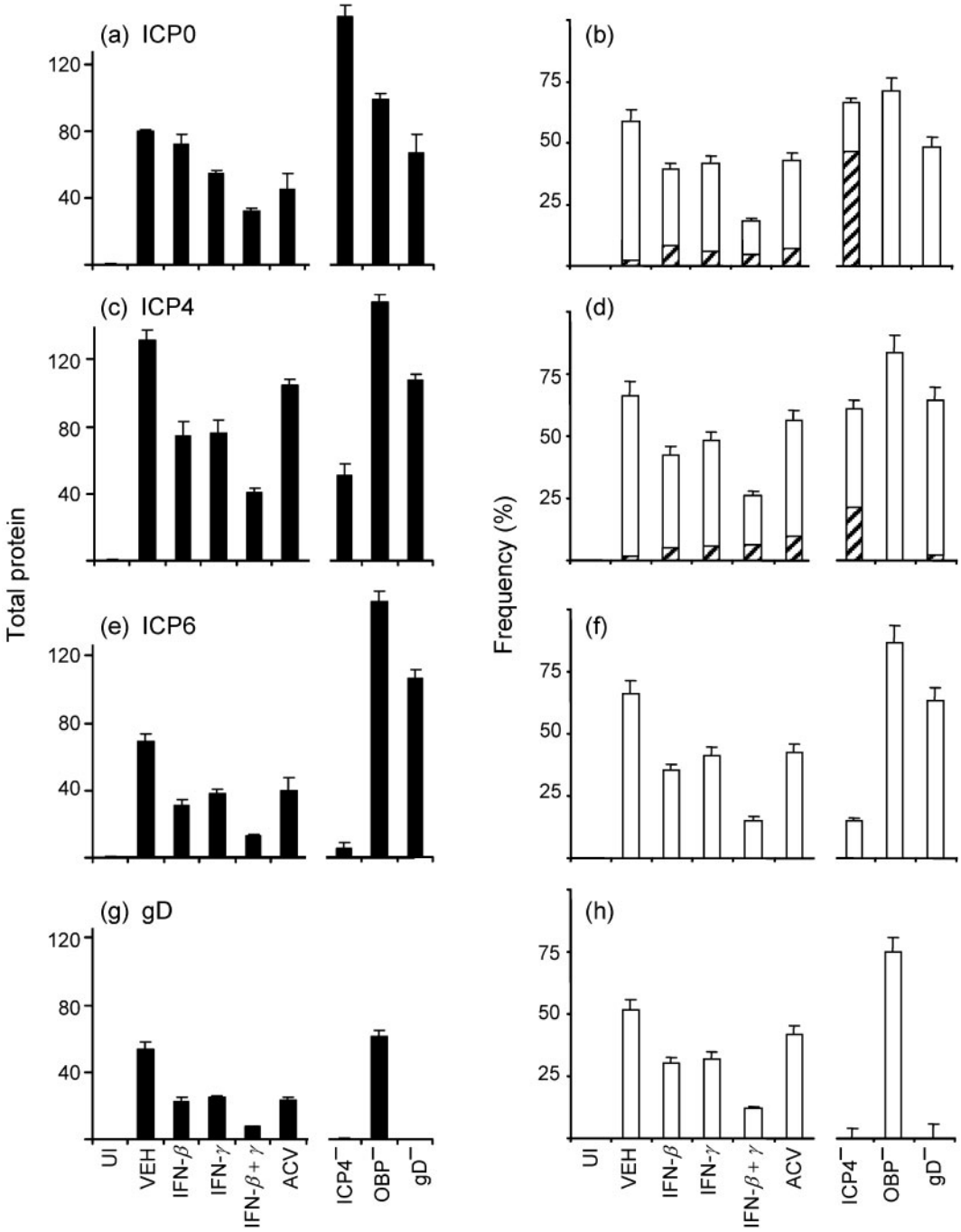

Fig. 4. Effect of IFN-β and IFN-γ on viral protein levels. Viral protein expression in uninfected Vero cells (UI) or in infected cells harvested 9 h after inoculation with 2·5 p.f.u. KOS, n12 (ICP4$^-$), hr94 (OBP$^-$) or KOS-gD6 (gD$^-$) per cell. The total abundance (a, c, e and g) versus frequency of viral protein-positive cells (b, d, f and h) was analysed by flow-cytometric measurement of the amount of ICP0, ICP4, ICP6 or gD present in 7000–9500 cells per culture ($n=3$ samples per group; 10 000 events per sample). KOS-infected cells were treated with vehicle (VEH), 200 U IFN-β ml^{-1}, 200 U IFN-γ ml^{-1}, 100 U each of IFN-β and IFN-γ ml^{-1} or 300 μM ACV. (a, c, e, g) Filled bars and error bars indicate the mean ± SEM of measurements of total protein abundance, which are expressed in terms of fold increase above the lower limit of detection of the assay, which was assigned a value of 1 ($n=3$ per group). (b, d, f, h) The frequency of viral protein-positive cells is represented as the fraction of cells that were labelled singly by mouse monoclonal anti-ICP0 (b), -ICP4 (d), -ICP6 (f) or -gD (h) only (hatched bars) versus cells that were labelled doubly with mouse mAb and rabbit polyclonal anti-HSV-1 (empty bars). Error bars indicate the mean coefficient of variation for the two subpopulations.

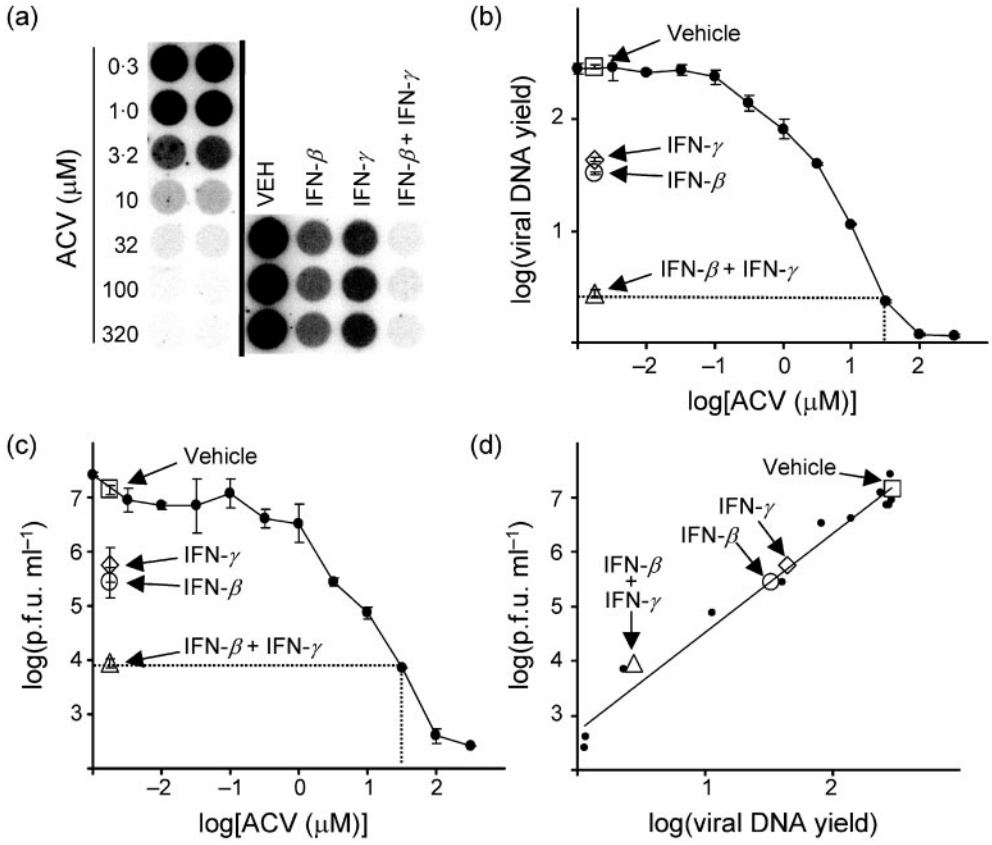

Fig. 5. IFN-β and IFN-γ inhibit HSV-1 replication before or during viral DNA synthesis. (a) Dot blot of Vero cell DNA harvested at 18 h after infection with 2·5 p.f.u. KOS per cell and hybridized to a US6-specific probe. KOS-infected cells were treated with vehicle (VEH), 200 U IFN-β ml^{-1}, 200 U IFN-γ ml^{-1}, 100 U each of IFN-β and IFN-γ ml^{-1} or 0·3–320 μM ACV. (b) Viral DNA yield as a function of ACV concentration (●; $n=2$ per dose). Viral DNA yields observed in cells treated with vehicle, IFN-β, IFN-γ or IFN-β and IFN-γ are shown on left side of the graph ($n=3$ each). Dashed lines indicate viral DNA yield in cells treated with IFN-β and IFN-γ and the ACV dose that reduced viral DNA to the same extent. (c) Viral titre as a function of ACV concentration (●; $n=2$ per dose). Viral titres recovered from cells treated with vehicle, IFN-β, IFN-γ or IFN-β and IFN-γ are plotted on the left side of the graph ($n=3$ each). Dashed lines indicate the viral titre in cells treated with IFN-β and IFN-γ and the ACV dose that reduced viral titre to the same extent. (d) Correlation of viral DNA yield and viral titre recovered from infected cells treated with ACV (●) versus cells treated with vehicle, IFN-β, IFN-γ or IFN-β and IFN-γ. The solid line indicates the line of regression between viral titres and viral DNA yield in ACV treatments ($r^2=0·97$).

inoculated with HSV-1 strain KOS (m.o.i. of 2·5) and harvested at 18 h p.i. Cellular sections were analysed by transmission electron microscopy. No structures resembling nucleocapsids or enveloped virions were observed in uninfected cells or KOS-infected cells treated with 300 μM acyclovir (not shown). In KOS-infected cells treated with vehicle, enveloped virions were apparent on most cell surfaces (Fig. 6a). Treatment with IFN-β or IFN-γ alone reduced the nucleocapsid density per cell, but viral particles were still evident in >95 % of cell sections (Fig. 6b and c). In contrast, treatment with IFN-β and IFN-γ inhibited virion formation and preserved the ultrastructural features of these cells (e.g. the intact Golgi apparatus in Fig. 6d). Fewer than 3 % of sections from cells treated with IFN-β and IFN-γ contained visible evidence of infection. In the few cells in which virus was observed, only one to five enveloped virions were observed in the cytoplasm or at the cell surface (Fig. 6d).

The combined versus separate effects of IFN-β and IFN-γ on HSV-1 virion yield were enumerated. At 18 h p.i., cells from each treatment group were subjected to freeze–thaw and the released virions were purified over a series of two discontinuous sucrose gradients. Fractions from the interface between the 30 and 60 % layers of the second gradient were used as coating antigens in an ELISA and the capacity of each fraction to capture polyclonal anti-HSV-1 antibody was measured (Fig. 7a). The results of two independent experiments demonstrated that the yield of HSV-1 virions in vehicle-treated cells was ~225 times

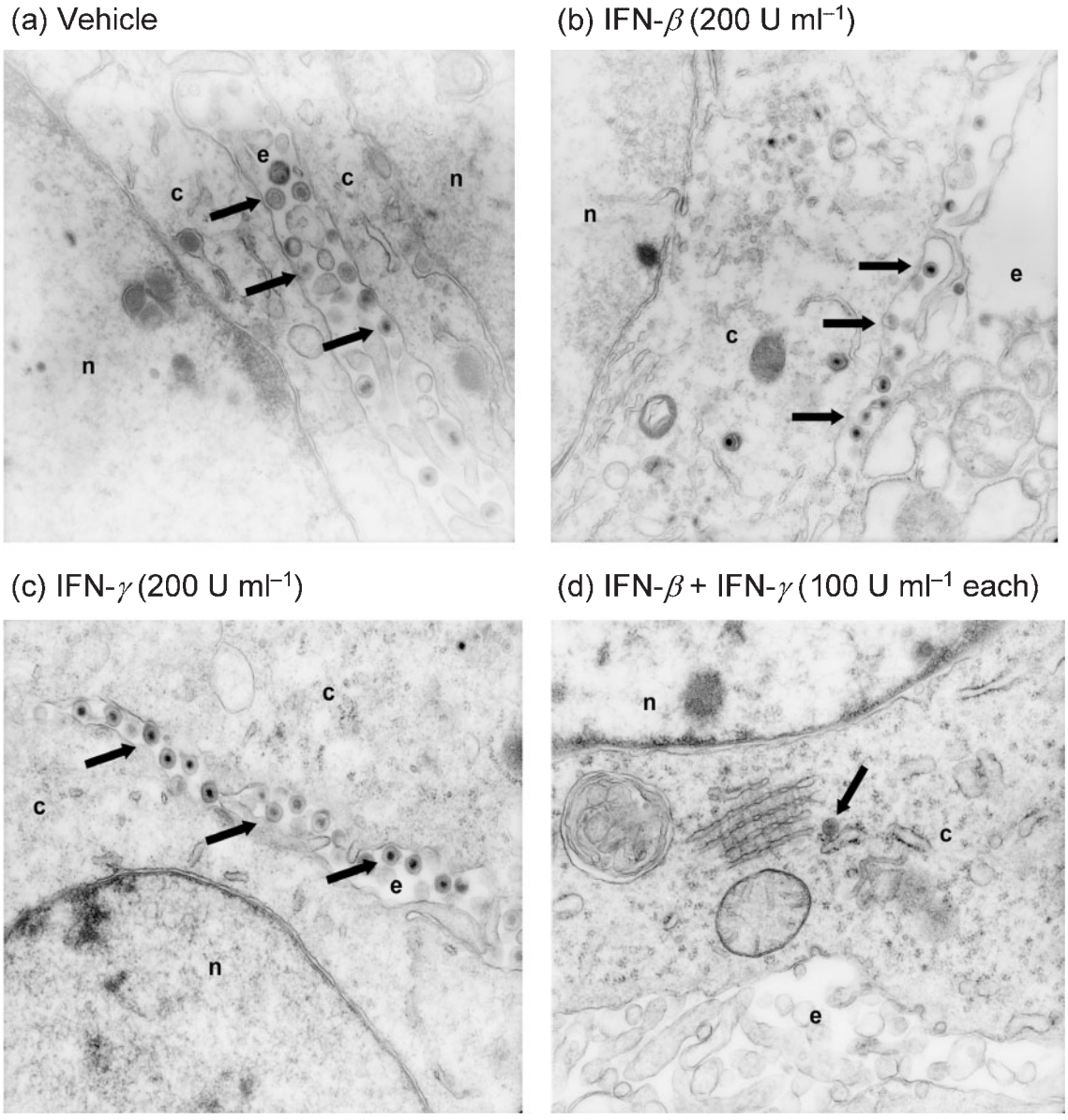

Fig. 6. Effect of IFN-β and IFN-γ on virion formation in HSV-1 infected cells. Electron micrographs of Vero cells harvested at 18 h after infection with 2·5 p.f.u. KOS per cell and treated with (a) vehicle, (b) 200 U IFN-β ml^{-1}, (c) 200 U IFN-γ ml^{-1} or (d) 100 U each of IFN-β and IFN-γ ml^{-1}. Arrows denote areas containing virus particles. n, Nucleus; c, cytoplasm; e, extracellular space.

greater than the background level of the assay (Fig. 7b). The yield of HSV-1 virions obtained from cells treated with IFN-β or IFN-γ was 29 and 46 % of that recovered from vehicle-treated cells, respectively (Fig. 7b). In contrast, in cells treated with IFN-β and IFN-γ, HSV-1 virion yield was only 2 % of that recovered from vehicle-treated cells (Fig. 7b). Therefore, combinations of IFN-β and IFN-γ repressed HSV-1 virion synthesis to a much greater extent than could be achieved with either IFN-β or IFN-γ alone.

DISCUSSION

IFN-β and IFN-γ do not compromise cell viability

Combinations of IFN-β and IFN-γ were not toxic to Vero cells, nor did these cytokines prime Vero cells to undergo virus-induced apoptosis. On the contrary, IFN-β and IFN-γ delayed the onset of viral CPE in HSV-1-infected cultures as measured by the preservation of (i) cellular morphology, (ii) cellular G3PDH mRNA levels and (iii) ultrastructural

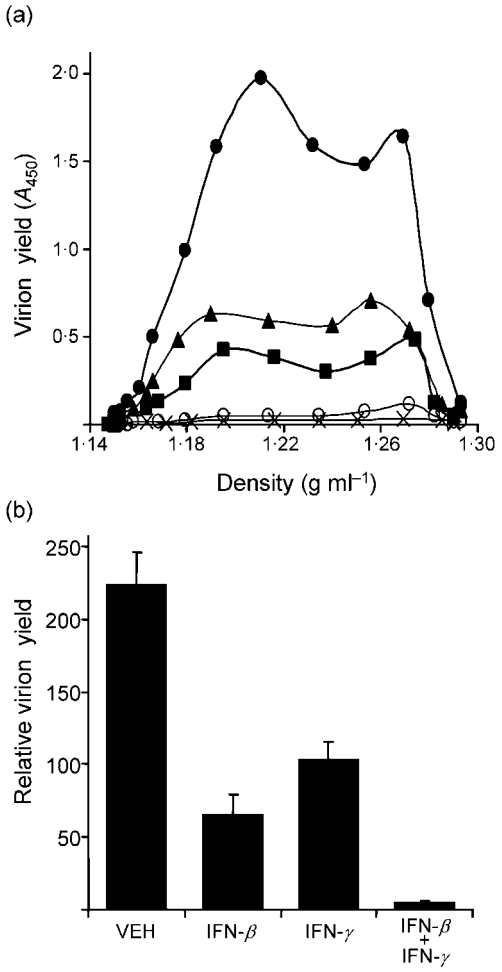

Fig. 7. Effect of IFN-β and IFN-γ on virion yield. (a) Virion yield in sucrose-gradient fractions, as determined by ELISA, plotted as a function of the A_{450} of each fraction. Virions were purified from Vero cells harvested at 18 h after infection with 2·5 p.f.u. KOS per cell and treated with vehicle (●), 200 U IFN-β ml^{-1} (■), 200 U IFN-γ ml^{-1} (▲), 100 U each of IFN-β and IFN-γ ml^{-1} (○) or 300 μM ACV (×). Uninfected cells processed in parallel were used to define the background of the ELISA. (b) Virion yield from cells treated with vehicle, IFN-β, IFN-γ, or IFN-β and IFN-γ. Shaded bars and error bars indicate the mean ± SD of the summation of virion yields measured by ELISA, which are expressed in terms of fold increase above the lower limit of detection of the assay ($n = 2$ independent experiments).

morphology. Therefore, we inferred that combinations of IFN-β and IFN-γ suppressed HSV-1 replication non-cytolytically via the disruption of productive virus replication.

Are the effects of IFN-β and IFN-γ on HSV-1 replication synergistic?

Pharmacological analysis of synergy focuses on differentiating whether an observed change in effect is due to (i) a cooperative interaction between two biologically active agents or (ii) the change in concentration that occurs whenever two agents are combined. Under a null hypothesis of dose additivity, IFN-β and IFN-γ would be assumed to have purely redundant effects, such that 100 U each of IFN-β and IFN-γ ml^{-1} should inhibit any step of HSV-1 replication to the average level of that achieved by 200 U IFN-β ml^{-1} or 200 U IFN-γ ml^{-1} (Tallarida, 2001; Tallarida *et al.*, 1997). The observed effects of IFN-β and IFN-γ were compared with the predictions of the null hypothesis (Table 1). In each case, IFN-β and IFN-γ reduced the synthesis of viral proteins, viral DNA and virions to an extent far greater than that predicted by the null hypothesis. Thus, the block in HSV-1 replication that was produced by co-activation of the IFN-α/β and IFN-γ pathways was quantitatively distinct from that which occurred when only one of these two signalling pathways was activated. The multiplicative nature of the interaction between the IFN-α/β and IFN-γ pathways is considered in detail elsewhere (Halford *et al.*, 2005a).

Where do IFN-β and IFN-γ act to inhibit HSV-1 replication?

Viral mutants or acyclovir were used to help break down the complex process of HSV-1 replication into discernible phases. The phenotypes that followed from failure to exit the IE phase of gene expression were defined by the ICP4$^-$ virus, n12 (DeLuca *et al.*, 1985). The consequences of a block in viral DNA synthesis were defined by the OBP$^-$ virus hr94 (Malik *et al.*, 1992) or treatment of KOS-infected cells with 300 μM acyclovir (Elion, 1983).

Inhibition of viral IE gene expression? Cells infected with an ICP4$^-$ virus expressed five times as much ICP0 as KOS-infected cells treated with IFN-β and IFN-γ. However, ICP4$^-$ virus-infected cells expressed low levels of ICP6 and undetectable levels of gD. In contrast, KOS-infected cells treated with IFN-β and IFN-γ exhibited a more gradual attenuation of E and L protein synthesis (i.e. ICP6, ICP8, gC and gD). Relative to the ICP4$^-$ virus, viral E and L proteins were far too abundant in IFN-treated, KOS-infected cells for repression of viral IE protein synthesis to be the sole mechanism by which IFN-β and IFN-γ inhibit HSV-1 replication.

Inhibition of viral DNA synthesis? IFN-β and IFN-γ did not block viral DNA synthesis in KOS-infected cells with the efficiency of 300 μM acyclovir. However, IFN-β and IFN-γ caused a greater reduction in viral IE and E protein synthesis than acyclovir treatment of KOS-infected cells. Likewise, an OBP$^-$ virus expressed high levels of ICP0, ICP4, ICP6 and ICP8, despite a complete block in viral DNA synthesis. Relative to these controls, viral IE and E protein expression was far too restricted in IFN-treated, KOS-infected cells for repression of viral DNA synthesis to be the sole mechanism by which IFN-β and IFN-γ inhibited HSV-1 replication.

Table 1. IFN-β and IFN-γ synergistically inhibit multiple steps in HSV-1 replication

Measure of HSV-1 replication	Fold reduction			Predicted dose-additive effect*	H_0: $\underline{P}-\underline{O}=0$†
	IFN-β (200 U ml^{-1})‡	IFN-γ (200 U ml^{-1})§	IFN-β+IFN-γ (100 U ml^{-1} each)‖		
ICP0 (IE)¶	1·1±0·1	1·5±0·0	2·5±0·2	1·3±0·1	$P<0·01$
ICP4 (IE)¶	1·8±0·2	1·7±0·2	3·3±0·2	1·8±0·2	$P<0·001$
ICP6 (E)¶	2·2±0·2	1·8±0·1	5·1±0·3	2·0±0·2	$P<0·01$
ICP8 (E)#	2·5±0·2	2·5±0·2	6·6±0·5	2·5±0·1	$P<0·05$
gC (L)¶	5·1±0·2	2·1±0·1	27±5	3·5±0·1	$P<0·05$
gD (L)¶	2·4±0·3	2·1±0·1	7·0±0·4	2·3±0·2	$P<0·01$
Viral DNA yield**	8·9±0·1	6·6±0·2	106±6	7·8±0·1	$P<0·001$
Virion yield††	3·5±0·8	2·2±0·3	45±5	2·9±1·5	NA‡‡

*Predicted ($\underline{P}$) fold reduction achieved by IFN-β and IFN-γ relative to vehicle-treated controls, based on a null hypothesis that nothing more than a dose-additive effect occurs when IFN-β and IFN-γ are combined.
†Probability that nothing more than a dose-additive effect occurs when IFN-β and IFN-γ are combined. Determined by a paired *t*-test of the null hypothesis that predicted−observed fold reduction is equal to 0.
‡Fold reduction observed in KOS-infected cells treated with 200 U IFN-β ml^{-1} relative to vehicle-treated controls.
§Fold reduction observed in KOS-infected cells treated with 200 U IFN-γ ml^{-1} relative to vehicle-treated controls.
‖Observed ($\underline{O}$) fold reduction in KOS-infected cells treated with 100 U each of IFN-β and IFN-γ ml^{-1} relative to vehicle-treated controls.
¶Mean±SEM fold reduction in ICP0, ICP4, ICP6, gC or gD proteins at 9 h p.i. ($n=3$ per group). Based on flow-cytometric analysis of each protein using mouse mAbs as the primary label and FITC-labelled goat anti-mouse IgG as the secondary label. These conclusions are based on the data presented in Fig. 4 with the exception of the gC data, which are not shown. The kinetic class of each viral protein is indicated in parentheses (IE, E or L).
#Mean±SEM fold reduction in ICP8 protein at 9 h p.i. ($n=3$ per group). Based on flow-cytometric analysis using rabbit polyclonal anti-ICP8 as the primary label and PE-labelled donkey anti-rabbit IgG as the secondary label (data not shown).
**Mean±SEM fold reduction in relative DNA yield at 18 h p.i. ($n=3$ per group). Based on results presented in Fig. 5.
††Mean±SD fold reduction in virion yield at 18 h p.i. ($n=2$ per group). Based on results presented in Fig. 7.
‡‡NA, Not applicable. The number of independent tests ($n=2$) was insufficient for statistical comparison of the summed value of total virion yield by the paired *t*-test used in this table. It should be noted that an appropriate statistical analysis of the 30 gradient fractions tested per group (e.g. two-way ANOVA) would indicate that the null hypothesis, H_0: $\underline{P}-\underline{O}=0$, should be rejected.

IFN-β and IFN-γ do not inhibit HSV-1 at the same step in every infected cell. Flow-cytometric analysis of viral protein expression revealed that IFN-β and IFN-γ must inhibit KOS replication at at least two distinct points. The first point of inhibition produced by IFN-β and IFN-γ reduced the frequency of KOS-infected cells that expressed detectable levels of ICP0 by 70 % relative to vehicle-treated cells (Fig. 4). Because IFN-β and IFN-γ do not preclude viral entry (Sainz & Halford, 2002), we inferred that IFN-β and IFN-γ repressed viral ICP0 gene expression successfully in ~70 % of KOS-infected cells. Absence of ICP0 renders viral IE genes highly susceptible to repression by IFN-α/β (Härle *et al.*, 2002; Mossman *et al.*, 2000). Thus, whether or not ICP0 is synthesized may create two divergent outcomes of HSV-1 infection. Under this hypothesis, one would predict that, if IFN-β and IFN-γ repress the ICP0 gene in ~70 % of KOS-infected cells, then all viral IE and E gene expression will be repressed in this subpopulation of cells (Mossman *et al.*, 2000). However, if IFN-β and IFN-γ fail to repress the ICP0 gene in ~30 % of KOS-infected cells, the resulting ICP0 protein that is synthesized will destabilize IFN-induced repression of viral IE genes (Härle *et al.*, 2002) and thus allow virus replication to proceed beyond this first restriction point. Although this hypothesis is highly consistent with the results, its validity remains to be tested.

The second discernible point of inhibition produced by IFN-β and IFN-γ lies at the level of viral DNA synthesis. The

50- to 100-fold reduction in viral DNA synthesis that was produced by IFN-β and IFN-γ would not be predicted based on the fact that $\sim$25 % of KOS-infected cells (relative to vehicle-treated controls) expressed normal levels of the E proteins ICP6 and ICP8 at 9 h p.i. The underlying mechanism that accounts for the block in viral DNA synthesis induced by IFN-β and IFN-γ remains to be elucidated and will certainly be the focus of future investigation. Given the hypersensitivity of HSV-1 ICP34·5$^-$ mutants to IFN-α/β (Cerveny *et al.*, 2003; Mossman & Smiley, 2002), one intriguing possibility is that expression of the other major viral IFN antagonist, ICP34·5, is repressed synergistically by IFN-β and IFN-γ such that HSV-1 is rendered highly susceptible to a protein kinase-induced shutoff of L viral protein translation (Leib *et al.*, 2000). The validity of this specific hypothesis remains to be tested.

Effect on downstream steps of virus replication. IFN-β and IFN-γ did not appear to inhibit phases of HSV-1 replication beyond HSV-1 DNA synthesis, such as virion maturation or egress. Doses of acyclovir that inhibited viral DNA synthesis to the same extent as IFN-β, IFN-γ or IFN-β and IFN-γ reduced infectious viral titres to precisely the same extent as each IFN treatment. Given that acyclovir acts solely to inhibit HSV-1 DNA synthesis, these data suggest strongly that the full inhibitory effect of IFN-β and/or IFN-γ is achieved before or during the process of HSV-1 DNA synthesis.

Relevance of the experimental design

In nature, animals are first infected with a virus and then respond by secreting cytokines such as IFN-α/β or IFN-γ. Given the natural order of events, what natural process is being modelled when Vero cells are pre-treated with IFN-β and IFN-γ for 16 h prior to infection? At the time at which HSV-1 first infects an animal, IFNs are absent in host tissues and the first productive cycle of virus replication proceeds unhindered *in vivo*. However, the available evidence suggests that host IFNs play a pivotal role in restricting the efficiency with which each of the approximately ten subsequent cycles of virus replication proceed during a typical 7 day course of acute infection *in vivo* (Halford *et al.*, 2005b; Luker *et al.*, 2003; Vollstedt *et al.*, 2004). Thus, the natural process being modelled when Vero cells are pre-treated with IFN-β and IFN-γ relates to the pivotal role that host IFNs play in restricting HSV-1 spread within infected tissues *in vivo*.

Conclusion

Co-activation of the IFN-α/β and IFN-γ signalling pathways produces a multiplicative inhibition of HSV-1 replication (Halford *et al.*, 2005a). Studies in IFN-receptor knockout mice corroborate the functional relevance of this interaction *in vivo* (Luker *et al.*, 2003; Vollstedt *et al.*, 2004). Given the persistence of IFN-γ-expressing CD8$^+$ T cells at sites of latent HSV-1 infection (Khanna *et al.*, 2003; Theil *et al.*, 2003), these results suggest that IFN-γ secretion may contribute to the capacity of CD8$^+$ T cells to protect HSV-1-infected neurons from viral CPE (Simmons & Tscharke, 1992). Although the current study offers only limited insight into the real mechanism of IFN-induced inhibition of HSV-1 replication, the results provide an empirical basis to focus on the relevant possibilities. We conclude that any viable hypothesis must be constrained by the facts that co-activation of the IFN-α/β and IFN-γ signalling pathways (i) does not compromise host-cell viability, (ii) prevents detectable viral IE and E protein synthesis in two-thirds of HSV-1-infected cells, (iii) blocks viral DNA synthesis in the remaining one-third of HSV-1-infected cells and (iv) effectively prevents the synthesis of new infectious virions.

ACKNOWLEDGEMENTS

This work was supported by grants from the National Institute of Allergy and Infectious Disease (R01 AI51414) and the National Center for Research Resources (P20 RR-020185-01). W. P. H. is supported by a National Science Foundation EPSCoR grant to Montana State University (EPS 0346458) and the Montana Agricultural Experiment Station. The authors extend their thanks to Carla Weisend for excellent technical assistance and to Bryan Gebhardt and Joel Graff for critical evaluation of this manuscript.

REFERENCES

Balish, M. J., Abrams, M. E., Pumfery, A. M. & Brandt, C. R. (1992). Enhanced inhibition of herpes simplex virus type 1 growth in human corneal fibroblasts by combinations of interferon-α and -γ. *J Infect Dis* **166**, 1401–1403.

Cerveny, M., Hessefort, S., Yang, K., Cheng, G., Gross, M. & He, B. (2003). Amino acid substitutions in the effector domain of the $\gamma_1$34.5 protein of herpes simplex virus 1 have differential effects on viral response to interferon-α. *Virology* **307**, 290–300.

Chen, S. H., Oakes, J. E. & Lausch, R. N. (1994). Synergistic anti-herpes effect of TNF-α and IFN-γ in human corneal epithelial cells compared with that in corneal fibroblasts. *Antiviral Res* **25**, 201–213.

DeLuca, N. A. & Schaffer, P. A. (1987). Activities of herpes simplex virus type 1 (HSV-1) ICP4 genes specifying nonsense peptides. *Nucleic Acids Res* **15**, 4491–4511.

DeLuca, N. A., McCarthy, A. M. & Schaffer, P. A. (1985). Isolation and characterization of deletion mutants of herpes simplex virus type 1 in the gene encoding immediate-early regulatory protein ICP4. *J Virol* **56**, 558–570.

Desloges, N., Rahaus, M. & Wolff, M. H. (2005). Role of the protein kinase PKR in the inhibition of varicella-zoster virus replication by beta interferon and gamma interferon. *J Gen Virol* **86**, 1–6.

Elion, G. B. (1983). The biochemistry and mechanism of action of acyclovir. *J Antimicrob Chemother* **12** (Suppl. B), 9–17.

Foster, T. P., Rybachuk, G. V., Alvarez, X., Borkhsenious, O. & Kousoulas, K. G. (2003). Overexpression of gK in gK-transformed cells collapses the Golgi apparatus into the endoplasmic reticulum inhibiting virion egress, glycoprotein transport, and virus-induced cell fusion. *Virology* **317**, 237–252.

Foster, T. P., Melancon, J. M., Baines, J. D. & Kousoulas, K. G. (2004). The herpes simplex virus type 1 UL20 protein modulates membrane fusion events during cytoplasmic virion morphogenesis and virus-induced cell fusion. *J Virol* **78**, 5347–5357.

Halford, W. P., Halford, K. J. & Pierce, A. T. (2005a). Mathematical analysis demonstrates that interferons-β and -γ interact in a multiplicative manner to disrupt herpes simplex virus replication. *J Theor Biol* **234**, 439–454.

Halford, W. P., Maender, J. L. & Gebhardt, B. M. (2005b). Re-evaluating the role of natural killer cells in innate resistance to herpes simplex virus type 1. *Virol J* (in press).

Härle, P., Sainz, B., Jr, Carr, D. J. J. & Halford, W. P. (2002). The immediate-early protein, ICP0, is essential for the resistance of herpes simplex virus to interferon-α/β. *Virology* **293**, 295–304.

Hubenthal-Voss, J., Houghten, R. A., Pereira, L. & Roizman, B. (1988). Mapping of functional and antigenic domains of the α4 protein of herpes simplex virus 1. *J Virol* **62**, 454–462.

Khanna, K. M., Bonneau, R. H., Kinchington, P. R. & Hendricks, R. L. (2003). Herpes simplex virus-specific memory $CD8^+$ T cells are selectively activated and retained in latently infected sensory ganglia. *Immunity* **18**, 593–603.

Leib, D. A., Machalek, M. A., Williams, B. R. G., Silverman, R. H. & Virgin, H. W. (2000). Specific phenotypic restoration of an attenuated virus by knockout of a host resistance gene. *Proc Natl Acad Sci U S A* **97**, 6097–6101.

Luker, G. D., Prior, J. L., Song, J., Pica, C. M. & Leib, D. A. (2003). Bioluminescence imaging reveals systemic dissemination of herpes simplex virus type 1 in the absence of interferon receptors. *J Virol* **77**, 11082–11093.

Malik, A. K., Martinez, R., Muncy, L., Carmichael, E. P. & Weller, S. K. (1992). Genetic analysis of the herpes simplex virus type 1 UL9 gene: isolation of a *lacZ* insertion mutant and expression in eukaryotic cells. *Virology* **190**, 702–715.

Mossman, K. L. & Smiley, J. R. (2002). Herpes simplex virus ICP0 and ICP34.5 counteract distinct interferon-induced barriers to virus replication. *J Virol* **76**, 1995–1998.

Mossman, K. L., Saffran, H. A. & Smiley, J. R. (2000). Herpes simplex virus ICP0 mutants are hypersensitive to interferon. *J Virol* **74**, 2052–2056.

Park, S.-Y., Seol, J.-W., Lee, Y.-J. & 9 other authors (2004). IFN-γ enhances TRAIL-induced apoptosis through IRF-1. *Eur J Biochem* **271**, 4222–4228.

Poon, A. P. W., Silverstein, S. J. & Roizman, B. (2002). An early regulatory function required in a cell type-dependent manner is expressed by the genomic but not the cDNA copy of the herpes simplex virus 1 gene encoding infected cell protein 0. *J Virol* **76**, 9744–9755.

Sainz, B., Jr & Halford, W. P. (2002). Alpha/beta interferon and gamma interferon synergize to inhibit the replication of herpes simplex virus type 1. *J Virol* **76**, 11541–11550.

Sainz, B., Jr, Mossel, E. C., Peters, C. J. & Garry, R. F. (2004). Interferon-beta and interferon-gamma synergistically inhibit the replication of severe acute respiratory syndrome-associated coronavirus (SARS-CoV). *Virology* **329**, 11–17.

Sainz, B., Jr, LaMarca, H. L., Garry, R. F. & Morris, C. A. (2005). Synergistic inhibition of human cytomegalovirus replication by interferon-alpha/beta and interferon-gamma. *Virol J* **2**, 14.

Schang, L. M., Phillips, J. & Schaffer, P. A. (1998). Requirement for cellular cyclin-dependent kinases in herpes simplex virus replication and transcription. *J Virol* **72**, 5626–5637.

Simmons, A. & Tscharke, D. C. (1992). Anti-CD8 impairs clearance of herpes simplex virus from the nervous system: implications for the fate of virally infected neurons. *J Exp Med* **175**, 1337–1344.

Smith, K. O. (1964). Relationship between the envelope and the infectivity of herpes simplex virus. *Proc Soc Exp Biol Med* **115**, 814–816.

Soboleski, M. R., Oaks, J. & Halford, W. P. (2005). Green fluorescent protein is a quantitative reporter of gene expression in individual eukaryotic cells. *FASEB J* **19**, 440–442.

Takaoka, A., Hayakawa, S., Yanai, H. & 8 other authors (2003). Integration of interferon-α/β signalling to p53 responses in tumour suppression and antiviral defence. *Nature* **424**, 516–523.

Tallarida, R. J. (2001). Drug synergism: its detection and applications. *J Pharmacol Exp Ther* **298**, 865–872.

Tallarida, R. J., Stone, D. J., Jr & Raffa, R. B. (1997). Efficient designs for studying synergistic drug combinations. *Life Sci* **61**, PL417–PL425.

Theil, D., Derfuss, T., Paripovic, I., Herberger, S., Meinl, E., Schueler, O., Strupp, M., Arbusow, V. & Brandt, T. (2003). Latent herpesvirus infection in human trigeminal ganglia causes chronic immune response. *Am J Pathol* **163**, 2179–2184.

Vollstedt, S., Arnold, S., Schwerdel, C., Franchini, M., Alber, G., Di Santo, J. P., Ackermann, M. & Suter, M. (2004). Interplay between alpha/beta and gamma interferons with B, T, and natural killer cells in the defense against herpes simplex virus type 1. *J Virol* **78**, 3846–3850.

Warner, M. S., Geraghty, R. J., Martinez, W. M., Montgomery, R. I., Whitbeck, J. C., Xu, R., Eisenberg, R. J., Cohen, G. H. & Spear, P. G. (1998). A cell surface protein with herpesvirus entry activity (HveB) confers susceptibility to infection by mutants of herpes simplex virus type 1, herpes simplex virus type 2, and pseudorabies virus. *Virology* **246**, 179–189.